Evaluation of tensile strength retention and service life prediction of hydrothermal aged balanced orthotropic carbon/glass and Kevlar/glass fabric reinforced polymer hybrid composites

M. Muralidharan[1], T. P Sathishkumar[2,*], N. Rajini[3,*], P. Navaneethakrishnan[2], S. Ramakrishnan[2], Sikiru O. Ismail[4], K. Senthilkumar[5], Suchart Siengchin[5]

[1, 2] Department of Mechanical Engineering, Kongu Engineering college, Perundurai, Erode, Tamilnadu, India

[3] Department of Mechanical Engineering, Kalasalingam Academy of Research and Education, Krishnankoil 626126, Tamilnadu, India.

[4]Department of Engineering, School of Physics, Engineering and Computer Science, University of Hertfordshire, Hatfield, AL10 9AB, Hertfordshire, England, United Kingdom.

[5]Department of Materials and Production Engineering, The Sirindhorn International Thai-German Graduate School of Engineering (TGGS), King Mongkut's University of Technology North Bangkok, 1518 Wongsawang Road, Bangsue, Bangkok 10800, Thailand.

[*]**Corresponding authors:**

T. P. Sathiskumar, E-mail: tpsathish@kongu.ac.in, Tel.: +91 9943570495

N. Rajini, Email: rajiniklu@gmail.com.

Abstract

Quest to reduce high structural weight and cost of metallic components, leading to their replacement with carbon and Kevlar fibers reinforced polymer (FRP) composites are increasing. These problems can be solved through hybridization of carbon/glass (CG) and Kevlar/glass (KG) fibers to reduce the manufacturing cost and materials usage, not at detriment of their properties. Therefore, investigation into their tensile properties, diffusivity and service life is germane. The present study focuses on influence of hybridization of carbon/glass and Kevlar/glass fibers on seawater diffusivity, service life and tensile strengths of their composite systems, through hydrothermal aging. The hybrid composites were aged in seawater for 50, 150 and 300 days at temperatures of 20, 40 and 60 °C. From the results obtained, it was evident that the maximum moisture absorption of both FRP hybrid composites occurred at 60 °C in 300 days of hydrothermal aging. The maximum tensile strengths were obtained in unaged composite counterparts. Also, the aged FRP hybrid composites exhibited the lowest tensile strengths at 150 days. The retention of maximum tensile strengths of CG and KG FRP hybrid composites showed 75 and 70% for 100 years at hydrothermal aging temperature of 40 °C. Therefore, both FRP hybrid composite samples exhibited promising behaviours for various marine applications.

Keywords: Tensile strength; hydrothermal aging; durability; service life; FRP hybrid composites.

1. Introduction

The use of synthetic fiber reinforced polymer (FRP) composites made of carbon, Kevlar and glass fibers are widely encouraged by researchers, academicians and industrialists, due to their lightweight, higher strength-to-weight, higher stiffness-to-weight, higher specific strength, relative less cost for making composites and higher durability. The high cost of carbon fiber reinforced polymer composites (CFRP) can be reduced by hybridization of carbon, glass and Kevlar fibers to achieve competitive structural properties [1,2]. From economical perspective, some glass fiber and Kevlar fiber reinforced polymer composite (GFRP and KFRP) components cannot be completely replaced by CFRP in automobile, aviation, earth moving, industrial machineries and marine applications. Alternatively, the secondary reinforcement of inorganic nanofillers, such as SiO_2 and $CoFe_2O_4$ [3], SiO_2 [4,5], Al_2O_3 [4–6], ATH [4,5], MgO [4,5], $CaCO_3$ [4,5], MgO [4,5], g-C3N4 [5], TiO_2 and Al_2O_3 [7], multi-walled carbon nanotubes [6,8,9] graphene oxide nanoplatelets [8,9], $BaTiO_3$ [10], SiC [6] and graphene-carbon nanotube [9] were added in GFRP and KFRP composites to increase their mechanical properties.

Also, the retention of mechanical properties under hydrothermal condition can be improved by addition of nano fillers [11–14] in GFRP composites. Then, the addition of nano fillers into GFRP and KFRP composites can marginally improve their mechanical properties [3,13]. Before using the aforementioned synthetic FRP composites in structural applications, scientists, industrialists and researchers are required to investigate their durability and retention of strengths through hydrothermal aging. It is therefore germane to obtain retention of mechanical, dynamics and thermal properties of these composites at different environmental conditions, such as normal, distilled, artificial salt, sea water and chemical solutions.

Carbon fiber/vinyl ester composite rods were shocked with NaCl solution and distilled water at 95 and 65 °C. The percentage of moisture absorption of composite in distilled water was obtained to be less than 0.6% when the composites were immersed in 3% NaCl solution at 65 °C. The flexural and interlaminar shear (mechanical) strengths were greater than 60% up to 1200 hours of hydrothermal aging at 3% NaCl solution, when compared with distilled water aged counterparts [15]. The damping factor (tan δ) peck was obtained to be less for unaged carbon fiber/vinyl ester composite rods. But, an increase in their aging times caused an increase in tan δ to higher values, and the maximum peak occurred at 1680 hours of aging in distilled water. This reduced the retention of dynamic properties [16]. The E-glass epoxy composite was hydrothermal aged at 75 °C from 0 to 1200 hours in water. The tensile strength, Poisson ratio and modulus of elasticity along longitudinal and transverse directions were gradually reduced by increasing the aging time. The maximum impact energy was obtained at 700 hours of aging and afterwards, the energy gradually declined [17].

Moreover, aging of CFRP composites in water at 80 °C for 8 hours with ultraviolet (UV) environment showed less interlaminar shear strength (ILSS) when compared with unaged composites [18]. The retention of ILSS of CFRP composites showed 74.5 and 50.0% at 500 and 1200 hours of hydrothermal aging at 70 °C, due to loss of bonding between their layers, which allowed rapid absorption of water by the composites. The percentage of ILSS retention was maintained as 40% constant after 1500 hours aging [19]. More also, GFRP composites were exposed to kerosene, biofuel and mixture of both at 24 °C for 1600 hours. The maximum tensile and compressive strengths were found in kerosene and biofuel aging [20]. Both increasing moisture absorption and decreasing mechanical properties were studied under various hydrothermal aging conditions [21]. The percentage of retention of various properties of CFRP and GFRP composites were predicted by varying temperature and time, using different solutions [22–29].

In addition, the seawater absorption of both CFRP and GFRP epoxy and vinyl ester composites were studied at 30 °C hydrothermal process. CFRP composites showed less water absorption than

GFRP counterparts. The percentage of change in mass was obtained to be less after 2 years of continuous aging [30]. The flexural strengths of CFRP vinyl ester composites were recorded to be high up to 200 days of aging and subsequently, the CFRP epoxy composites recorded high flexural strengths up to 450 days of aging. An opposite trend was exhibited by GFRP epoxy and vinyl ester composites [31]. The higher glass fiber volume fraction showed more water absorption and also recorded higher reduction of tensile and flexural strengths. Aging composites at 14, 28 and 42 days showed tensile strengths of 460, 442 and 429 MPa, respectively and flexural strengths of 389, 300 and 278 MPa, respectively [32]. GFRP composites were immersed in seawater at 40, 60 and 80 °C. An increase in temperature led to an increase in coefficient of diffusivity by absorbing more water. The moisture absorption was higher for artificial seawater than normal water [33]. The graphene oxide mixed GFRP epoxy composites showed less water absorption, because graphene resisted water uptake [34]. By comparing CFRP and GFRP composites under low velocity impact test, the impact load absorption against time and deflection were obtained to be higher for CFRP composites. Also, the similar trend was recorded in their tensile strengths [35].

To further improve the properties of FRP composites, hybrid composites were developed and their properties retention through hydrothermal aging process were studied. The E-glass and carbon FRP hybrid composites with three layering patterns showed that CG_3C pattern hybrid composites exhibited less water absorption. The mechanical properties were obtained to be less in aged composites, and the retention of tensile and flexural properties was higher in CFRP than GFPR composites [36]. Besides, GFRP pultruded composite was hydrothermally aged at 20, 40 and 60 °C for 12 months. The maximum flexural strength retention was obtained for isophthalic polyester GFRP composites and compared with orthophthalic and vinyl ester GFRP composites. The Arrhenius plots was used to predict the service life of the composites [37]. By increasing the use of hybrid composites in various engineering sectors, the long-term service life prediction is very important for structural requirement at user end.

Continuous characterization of different patterns of hybrid composites is necessary to obtain better properties of various FRP composites. The mechanical properties retention and service life predication are important recommended characteristics for newly developed FRP composites. Therefore, this present study aims at predicating tensile strength retention under seawater hydrothermal aging and service life of carbon/glass (CG) fibers and Kevlar/glass (KG) FRP hybrid composites at different environmental conditions, such as 20, 40 and 60 °C, aging periods of 50, 150 and 300 days. The Arrhenius methodology was used to predict the long-term service life characteristic of the FRP hybrid composites.

2. Materials and methods

Fig. 1 shows the methods and processes of preparing and characterizing the synthetic fibers reinforced epoxy hybrid composite samples used.

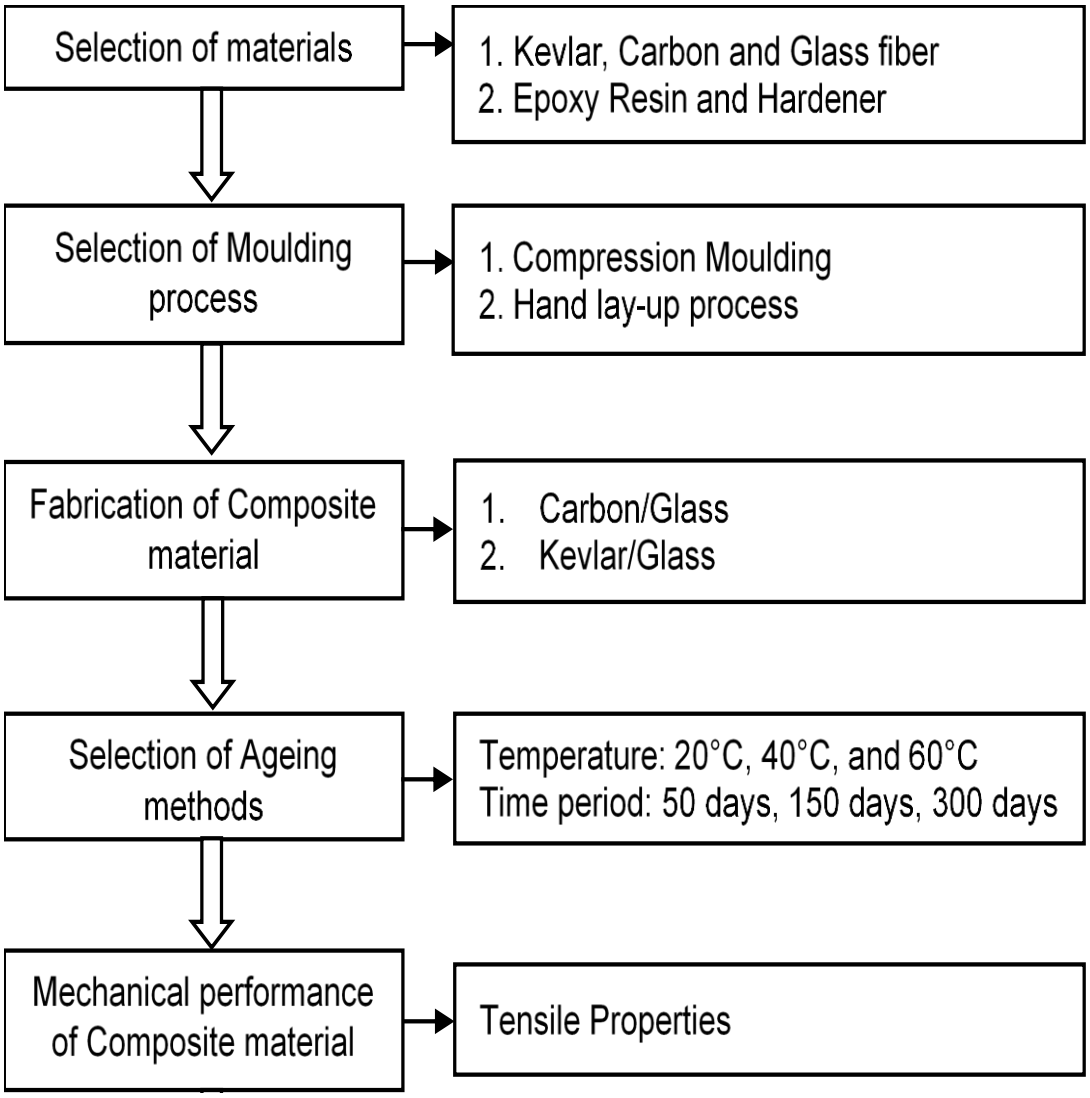

Fig. 1. Illustration of preparation and characterization processes of the hybrid composite samples.

2.1. Materials

Fiberglass, carbon and Kevlar fiber fabrics were purchased from Covai Senu industry, Coimbatore, Tamilnadu, India. Figs 2(a), (b) and (c) respectively show the glass, carbon and Kevlar fiber fabrics for the preparation of the hybrid composites. Table 1 represents the properties of the carbon, Kevlar and glass fibers used. The epoxy resin (LY556) and hardener (HY951) were purchased from the same fibers' supplier. The physico-mechanical properties of epoxy are presented in Table 2. It has good mechanical properties, adhesion with synthetic fibers and very less shrinkage when compared with other thermoset resins.

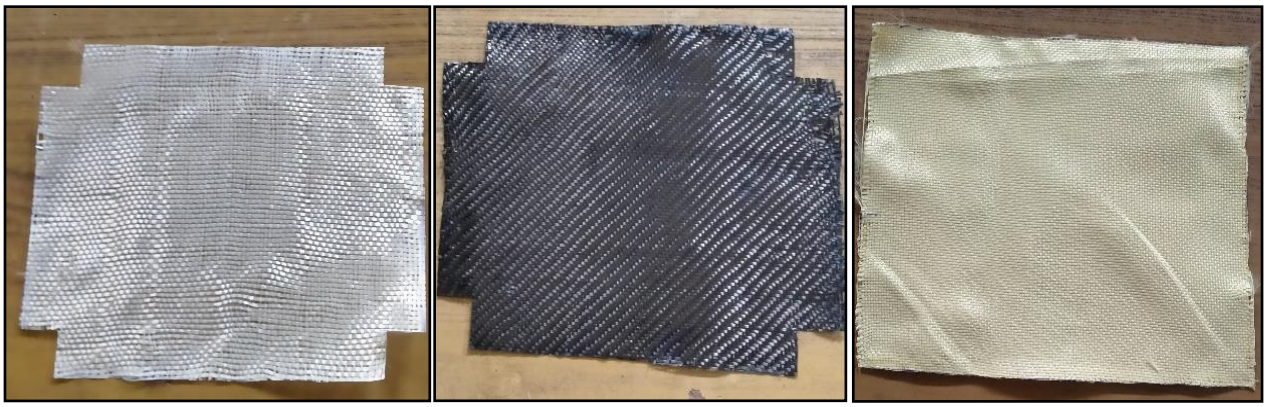

(a) Glass fiber fabric (b) Carbon fiber fabric. (c) Kevlar fiber fabric.

Fig. 2. Various synthetic fiber fabrics used.

Table 1

Properties of carbon, Kevlar and glass fibers used.

	Values		
Properties	E-glass fiber mat	Carbon fiber mat (E-75)	Kevlar fiber mat (K-29)
Density (g/cm³)	2.54	1.65	1.44
Tensile strength (MPa)	2200 ± 47	3190 ± 56	3620 ± 68
Young's modulus (GPa)	73 ± 3	228 ± 5	131 ± 8

Table 2

Physico-mechanical properties of epoxy used.

Properties	Values
Specific gravity at 25 °C	1.16 ± 0.02
Density (g/cm³)	1.16
Viscosity at 25 °C (cps)	1150
Tensile strength (MPa)	24
Tensile modulus (GPa)	0.5
Elongation (%)	2.5
Flexural strength (MPa)	45
Flexural modulus (MPa)	1.25
Equivalent weight of epoxy resin (EEW) g/eq.	178
Compression strength (MPa)	63

2.2. Preparation of laminated FRP hybrid composites

CG and KG fibers reinforced laminated epoxy hybrid composites were prepared by hand lay-up process coupled with compression molding method. Fig. 3 shows the order of laminating the balanced orthotropic laminas of CG and KG fibers into the composite systems. The layering patterns of C/G/C/G/C/G/C/G/C (C_5G_4) and K/G/K/G/K/G/K/G/K (K_5G_4), where C, K and G represent carbon, Kevlar and glass (Fig. 3) respectively, were used to prepare the laminated FRP hybrid composites according to the theory of composite systems. Fig. 4 additionally shows the stacking sequences of both CG and KG fiber fabrics for preparing the hybrid composites. The laminas of required size were cut from the long-fabric mat with dimension of 240 × 200 mm (Fig. 4). A steel plate mold was used to prepare the hybrid composites. Initially, the resin and hardener were mixed by using mechanical stirrer in ratio of 10:2 for 10 minutes and the releasing agent of liquid polyvinylchloride (PVC) was coated on the inside surface of the mold, which helped to easily remove the solidified composites. Before laminating, the laminas were completely dipped in resin solution for 1 minute and laid one-by-one on female die. A steel roller was used to roll over every lay-up to remove the air bubbles developed between the laminas and ensure an even distribution of resin over the layers. Totally, nine layers were used for the lamination; five layers of carbon and Kevlar fiber fabrics, each and four layers of glass fiber fabrics. Afterwards, the closed steel mold was kept in a hydraulic press with applied pressure of 25 bar for 6 hours at room temperature. Finally, the solidified composite plate was removed from the mold and preheated for 1 hour in a hot air oven at 45 °C to ensure complete curing or solidification.

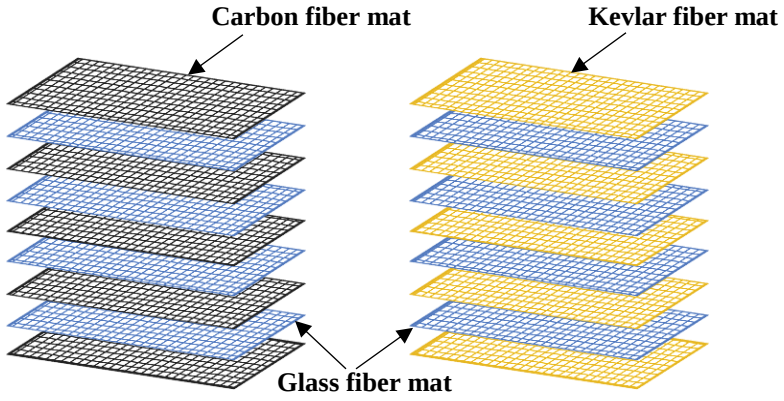

Fig. 3. Layeirng sequences of balanced orthotropic laminas of (a) carbon/glass (C_5G_4) and (b) Kevlar/glass (K_5G_4) FRP hybrid composites.

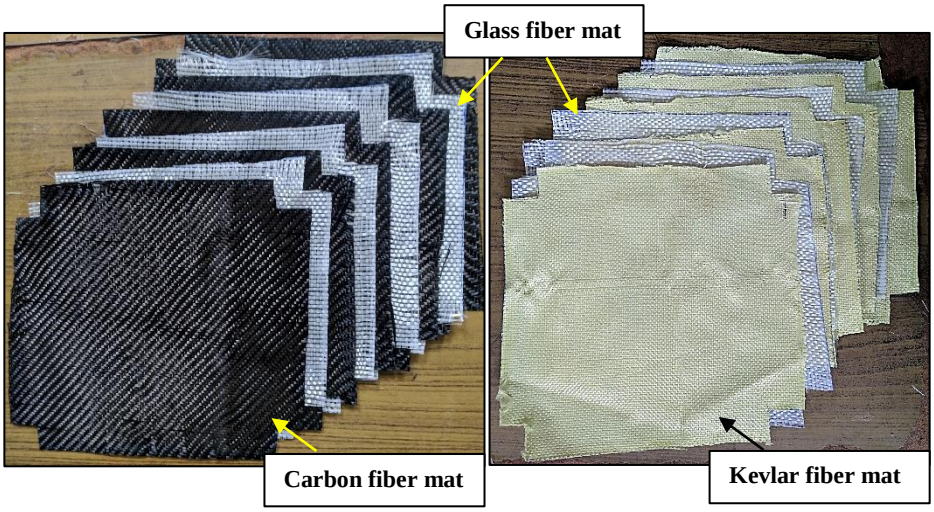

Fig. 4. CG (C_5G_4) and KG (K_5G_4) fiber fabrics for preparing FRP hybrid composites.

2.3. Aging of FRP hybrid composites

Hydrothermal aging process was performed to analyze the water absorption behaviors and calculate the weight gain of both composites, as a function of time. After aging, prediction of service life of the FRP hybrid composites was carried out based on the Arrhenius principle [23,37,38] and it helped to study the long-term behaviors of both CG and KG FRP hybrid composites. The tensile test samples of CG and KG composite samples were immersed in seawater at three different temperatures of 20, 40 and 60 °C to analyze their diffusivity, long-term tensile strength retention and service life. The cold-seawater aging at 20 °C was done by keeping a bowl of seawater with tensile test samples in refrigerator and maintained the temperature at 20 °C for entire immersion period. The hot-seawater aging at 40 and 60 °C was done by keeping all the samples in a water heater with aid of 60 watts U-type heating coil and thermostat. The aging periods were 50, 150 and 300 days for all environmental conditions. In hot-seawater aging, the apparatus was completely closed to avoid the excessive evaporation of seawater.

The temperature of seawater was maintained within a tolerance of ±2 °C with help of thermostat. Before aging, the weights of both composite samples were measured and recorded, using digital weighing machine with accuracy of 0.001 gram. The weights of aged samples were measured and recorded at regular intervals of 10 days for the testing periods of 50, 150 and 300 days. The percentage of weight variation (Δ_m) between the unaged and aged composites was calculated, using Eq. (1) [15,39].

$$\Delta_m = \left(\frac{m_t - m_o}{m_o}\right) x\ 100 \quad (1)$$

Where, m_t and m_o represent the masses of the samples at time *t* and initial state (gram), respectively.

2.4. Tensile test

Tensile test was conducted in accordance with ASTM D 638 standard with Type-1 sample size [40]. The dog-bone shaped tensile test samples were cut by using zig-zag machine. Figs 5(a) and (c) show the dog-bone shaped CG and KG FRP hybrid composite samples.

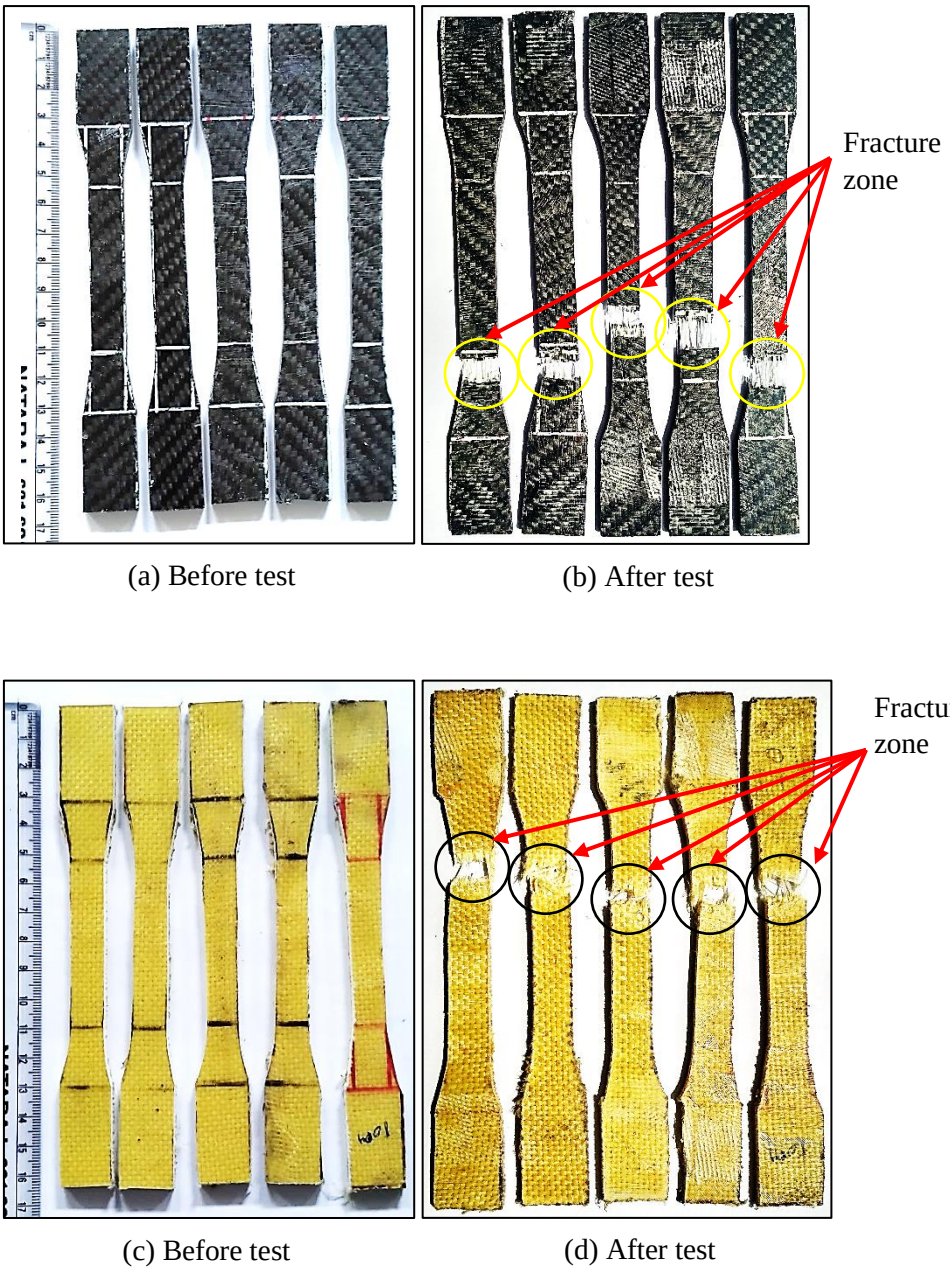

(a) Before test (b) After test

(c) Before test (d) After test

Fig. 5. Dog-bone shaped tensile test samples (a, c) before and (b, d) after test.

The dimension of each sample was 165 × 19 × 3 mm. The gauge length and width of each of the samples were 50.0 and 12.7 mm, respectively. The tensile test was conducted by using UTM with load cell of 30 kN and testing speed of 2 mm/min. Five identical samples were tested to obtain average values of properties. The tensile fracture appeared expectedly between the gauge length of the composite samples for all environmental conditions at various aging periods, as depicted in Figs

5(b) and (d). These were further elucidated later, under results and discussion section. Average values of tensile strengths obtained were calculated and taken for discussion. However, seven to eight samples were tested in a very few cases. The tensile stress *versus* tensile strain curves were recorded and the percentage of reduction and retention of tensile properties were determined.

2.5. Scanning electron microscope

Scanning electron microscope (SEM) was used to analyze the micro structural failures of fractured surfaces of CG and KG FRP hybrid composite samples through cross-section analysis method. This was carried out at Alagappa University, Karaikudi, Tamil Nadu, India. Before scanning, the fractured samples were cut into a length of 5 mm from the fractured point and coated with gold to capture clear image. The following specifications were used for scanning the image: resolution of 3.0 nm with AC V of 15 kV and WD of 8 to 9 mm, magnification from 50 to 500x and electron gun accelerating voltage of 0.5 to 30.0 kV.

2.6. Long-term performance prediction

Long-term tensile behaviors of the FRP hybrid composites were determined by using the Arrhenius principle. It is defined that the occurrence of material degradation depends on various environmental conditions, different temperatures and aging time periods [23,37,38]. Therefore, the service life of the composite samples was predicted by estimating the rate of degradation of tensile strength under various environmental conditions. The rate of degradation (k) was calculated, using Eq. (2) [23,37,38].

$$k = Ae^{\left(\frac{-E_a}{RT}\right)} \tag{2}$$

Where A = pre-exponential factor, T = temperature (Kelvin), E_a = activation energy (kJ/mol), R = Boltzman constant (1.38065×10^{-23} J/K). If k is known, the activation energy (E_a) can be calculated. The E_a shows the energy barrier of the composite materials. It was calculated from the diffusion coefficient, as subsequently represented in Eq. (7), which took place in the composite materials or samples during hydrothermal aging. The following relations (Arrhenius relationship) was used to calculate the E_a [23,37,38].

$$D = D_o exp\left(\frac{-E_a}{RT}\right) \tag{3}$$

Where, D = diffusion coefficient (mm^2/s), ($D = k$),

D_o = constant coefficient, ($D_o = A$),

R = universal gas constant equivalent (8.3144 J/mol K),

T = temperature of seawater aging (Kelvin).

Eq. 3 may be in another form, as shown in Eq. 4.

$$InD = -\left(\frac{-E_a}{R}\right)\left(\frac{1}{T}\right) + InD_o \tag{4}$$

Eq. (4) is a form of a straight-line equation; Eq. (5).

$$Y = mx + c \tag{5}$$

Where, $x = \frac{1}{T}$, $Y = InD$. Plot of natural log of (InD) *versus* $\frac{1}{T}$ gives straight-line equation. Therefore, the slope of linear fitting of line was used to calculate the E_a (kJ/mol), using Eq. (6). This equation is defined as $-R$ into the ratio of slope of InD *versus* $\frac{1}{T}$.

$$E_a = -R\left[\frac{\partial(InD)}{\partial(\frac{1}{T})}\right] \tag{6}$$

The diffusion coefficient (D) was calculated, using the Fick's law and considering the weight and time taken for moisture absorption and dimension of both composite samples. The Fick's law [11,16,19,28,31,32,36] relationship is given by Eq. (7).

$$D = \pi\left(\frac{h}{4M_m}\right)^2\left(\frac{M_2 - M_1}{\sqrt{t_2} - \sqrt{t_1}}\right)^2\left(1 + \frac{h}{l} + \frac{h}{n}\right)^{-2} \tag{7}$$

Where, h = thickness of the composite sample (mm),

l = length of the composite sample (mm),

n = width of the composite sample (mm),

M_m = maximum moisture absorption of the composite (gram),

M_1 and M_2 = moisture absorption of the composite sample (gram) at time t_1 and t_2 (sec).

3. Results and discussion

3.1. Aging behaviors

The percentages of weight gains by both CG and KG FRP hybrid composite samples under three different aging temperatures are shown in Fig. 6. Carbon/glass and Kevlar/glass fiber reinforced epoxy hybrid composites are respectively designated as CG and KG FRLEHC in all the subsequent relevant Figures. The five identical samples were taken out periodically to measure their percentages of weight gains and average values were calculated and discussed. The theoretical water absorption was predicted by using Eq. (7) and the results are presented as solid curves in Fig. 6. The

solid curves followed the Fickian behaviors, because the initial mass gain was rapidly increased [15], which later slowed down after prolonged seawater immersion.

From Fig. 6(a), the percentages of weight gains at 20 °C were 7.17±0.45 and 8.37±0.63% for CG and KG FRP hybrid composites at 50 days of aging, respectively. At 150 days, the percentage of weight gains were 9.96±0.53 and 12.35±0.65% for CG and KG FRP hybrid composites, respectively. At 300 days, the percentages of weight gains were 11.16±0.31 and 13.18±0.35% for CG and KG FRP hybrid composites, respectively. Evidently, the weight of both FRP hybrid composite samples increased rapidly at initial stage up to 75 days, obeying the Fickian behaviors and then it increased very slowly until it reached a saturation level. The CG FRP hybrid composite almost reached saturated level at 150 days of aging. By increasing the aging period up to 300 days, the rate of weight gain was very minimal when compared with before 150 days. It increased from 9.67 to 11.16%; improvement was 1.49%. Also, the KG FRP hybrid composites almost reached saturated level at 180 days of aging, and then an increase in the aging period gradually increased their percentages of weight gains. After 300 days of aging, the rate of weight gain was very minimum when compared with before 150 days; that is from 12.35 to 13.15%, the improvement was 0.8%. The CG FRP hybrid composites recorded less water absorption than KG counterparts at 20 °C. After 150 days, the rate of water absorption was decreased, hence the fiber-matrix debonding began and consequently degradation of composite materials occurred.

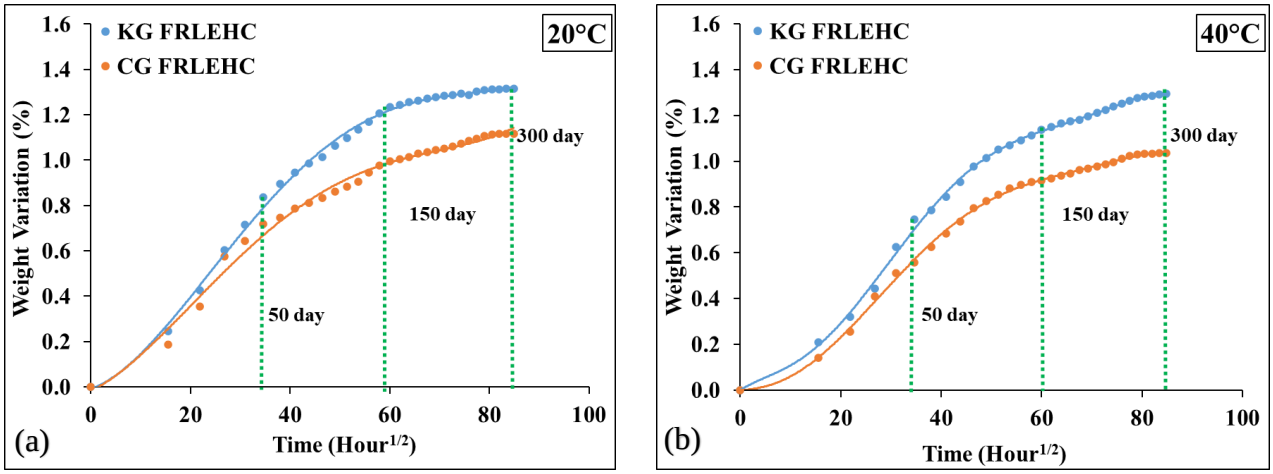

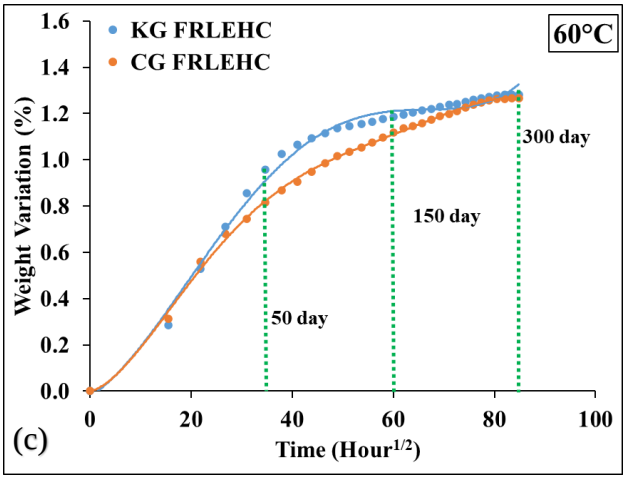

Fig. 6. Weight variation *versus* square root of time of CG and KG FRP hybrid composite samples immersed in water at (a) 20, (b) 40 and (c) 60 °C.

From Fig. 6(b), the percentages of weight gains at 40 °C were 5.58±0.32 and 7.45±0.37% for CG and KG FRP hybrid composites at 50 days of aging, respectively. At 150 days, the percentages of weight gains were 9.16±0.39 and 11.37±0.42% for CG and KG FRP hybrid composites, respectively. At 300 days, the percentages of weight gains were 10.36±0.38 and 12.94±0.40% for CG and KG FRP hybrid composites, respectively. The weight of both composite samples increased rapidly at the initial stage up to 100 days and then increased very slowly until it reached a saturation level. The CG FRP hybrid composites almost reached saturated level at 250 days of aging. After increasing the aging period up to 300 days, the rate of weight gain was very minimal when compared with 150 days. It increased from 11.37 to 12.65%; improvement was 1.28%. Also, KG composites reached saturated water gain at 270 days of aging, and then an increase in aging period gradually increased the percentage of weight gain. After 270 days of aging, the rate of weight gain was less when compared with 150 days that was from 11.37 to 12.94%, the improvement was 1.57%. The CG composites recorded less water absorption than KG composites, because carbon, Kevlar and glass fibers did not absorbed seawater, instead matrix only absorbed water [16]. After 150 days, the rate of water absorption by matrix was decreased, due to matrix degradation in both composite samples and consequently led to loss of fiber-matrix interfacial bonding.

From Fig. 6(c), the percentages of weight gains at 60 °C were 8.16±0.32 and 9.58±0.45% for CG and KG FRP hybrid composites after 50 days of aging, respectively. At 150 days, the percentage of weight gain were 11.186±0.41 and 11.85±0.47% for CG and KG FRP hybrid composites, respectively. A 300 days, the percentages of weight gains were 102.65±0.38 and 12.82±0.40% for CG and KG FRP hybrid composites, respectively. At 60 °C, the weights of both composite samples increased rapidly at the initial stage up to 150 days and then increased gradually until it reached a

saturation level. The CG composites almost reached saturated level at 270 days of aging. After increasing the aging period up to 300 days, the rate of weight gain was very minimal when compared with 150 days of 11.18 to 12.63%, improvement was 1.45%. Also, the KG composites reached saturated level at 280 days of aging. After 380 days of aging, the rate of weight gain was very minimal when compared with 150 days. It increased from 11.85 to 12.82%; improvement was 0.97%. The CG composites recorded less water absorption than KG counterparts at 60°C, because of the physical barrier between the carbon fiber and matrix. After 200 days, the rate of water absorption was decreased, due to degradation of matrix in both composite samples. Higher temperature of 60 °C degraded both composite samples at faster rate than the lower temperatures of 20 and 40 °C. The rate of absorption was higher at elevated temperature, which reduced the fiber-matrix bonding.

During hydrothermal aging, both CG and KG FRP hybrid composite samples were continuously absorbing heat. The presence of 4,4'-methylenedianiline (CH_3) group in epoxy chemical structure was weakening their bonding from ethylene oxide (O) groups at elevated temperature, because of the solubility of CH_3 in water at 20 °C to a room temperature. This deformed the cross link of chemical and shrunk the matrix at higher temperature and created small air gaps between the fiber and matrix surfaces. Also, due to heat, the Brownian motion of epoxy molecular chain of one oxygen and two carbon atoms was accelerated [28,32]. This resulted to an increase in the diffusivity and advanced the weakness of physical bonding between the fiber and matrix. Therefore, seawater penetrated into the micro cracks of the both composites and resulting in wicking on the fiber surface [31], which consequently reduced the mechanical properties of both composite samples. The GFRP composites absorbed seawater by almost 1.9 [34] and 3.0% [35], but hybridization of carbon and Kevlar fibers in GFRP composites showed lower seawater uptakes of 1.26 and 1.28%. It has been reported that seawater absorption/uptake by CG FRP hybrid composites was less than 1.15%, when compared with GFRP and CFRP composites at maximum aging period of 90 days [36].

3.2. Tensile properties

Fig. 7 shows tensile stress-strain curves of CG and KG FRP hybrid composite samples with and without aging, at different temperature of 20, 40 and 60 °C and time periods of 50, 150 and 300 days. The tensile stresses of all the samples were calculated, including their average values of loads, cross sectional areas, widths, gauge lengths and thicknesses. The width of the sample over the gauge length was 13 mm. The percentage of tensile strain was calculated as the ratio of elongation of the composite and sample gauge length of 50. The curve of the dry composite was compared with all

the curves of the wet composite samples. Figs 7(a), (c) and (e) show that the bilinear stress-strain curves were obtained for CG composites at dry and 50 days aged conditions, the slope increased linearly. At 150 days, the slope of the curves was non-uniformly increased up to final break. The progressive change in slope occurred at two stages of strain to the extent that the FRP hybrid composite samples began to degrade, due to water penetration into the composite samples. At 300 days aging, the slope of CG composite increased linearly for all temperatures, due to faster degradation of fiber-matrix interfacial bonding, caused by more water absorption. The strain to failure of aged composites was less when compared with the dry composite samples. The composites aged at 40 °C recorded the maximum stress-strain curve.

Moving forward, Figs 7(b), (d) and (f) show that the bilinear stress-strain curves were obtained from KG FRP hybrid composites at dry and aged conditions. For all curves, their slopes were linearly increased. By increasing the aging period, the strain rate was gradually decreased and the slopes of all the curves were linearly varied. At 150 and 300 days of aging, the tensile strain was observed equal for all environmental conditions. But, the composite samples started to degrade at 150 days. At 300 days of aging, the slope of KG FRP hybrid composite showed a perfect linear curve at 40 and 60 °C, due to more water penetration into the fiber-matrix interfaces of the composite samples. KG composites aged at 40°C exhibited the maximum stress-strain curve.

Also, Fig. 8 depicts the tensile properties, including tensile stresses, strains and moduli of both CG and KG FRP composites at three different temperatures and aging periods. Fig. 8(a) shows the tensile properties of aged composites at 20 °C. The tensile stresses of CG and KG FRP composites were 340.56 and 317.69 MPa at dry/unaged condition; for 0 day. After 50 days of aging, the tensile stresses of both CG and KG FRP hybrid composites were 315.69 and 268.00 MPa, respectively. The rate of reduction of tensile stresses of aged CG and KG FRP hybrid composites were nearly 7.0 and 15.5% (Fig. 9a), when compared with dry composites.

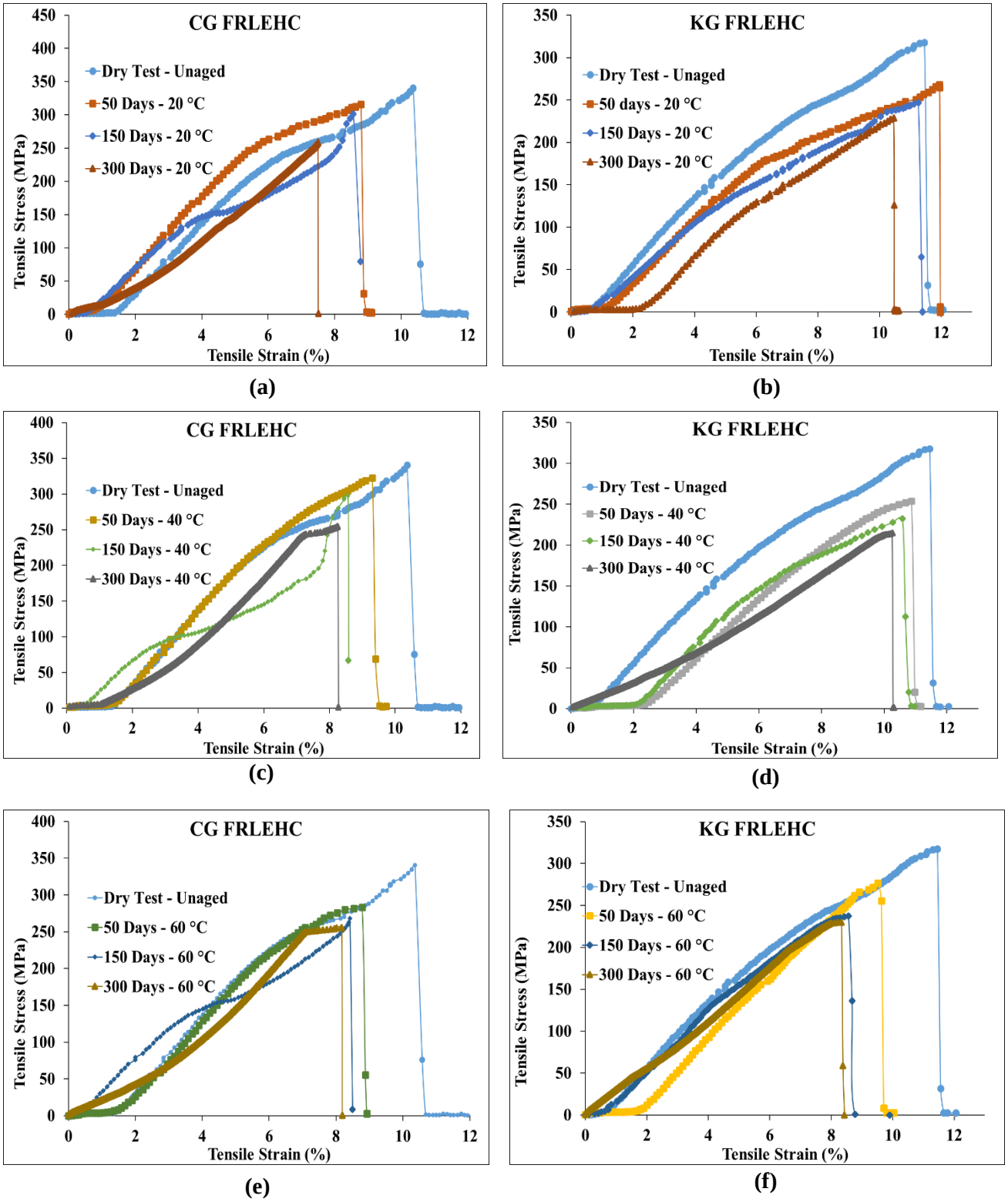

Fig. 7. Tensile stress *versus* tensile strain of dry/unaged and wet/aged CG and KG FRP hybrid composite samples immersed at different temperatures of (a, b) 20, (c, d) 40 and (e, f) 60 °C as well as aging periods of 50, 150 and 300 days.

Fig. 9 evidently shows that the tensile stresses of both composites constantly reduced, due to increase in time of exposure for all environments. After 150 days, the tensile stresses of both CG

and KG FRP hybrid composites were 301.25 and 246.79 MPa, respectively. Then, the rate of reduction of tensile stresses of aged CG and KG FRP hybrid composites were almost 11.50 and 22.30% (Fig. 9a), respectively. The percentage differences between 50 to 150 days were 4.6 and 8.0% for CG and KG FRP composite samples, respectively. After 300 days, the tensile stresses of both CG and KG FRP hybrid composites were 258.26 and 228.67 MPa, respectively. Furthermore, the rate of reduction of tensile stresses of aged CG and KG FRP hybrid composites were approximately 24.08 and 28.01% respectively (Fig. 9a), when compared with dry composites. The percentage reduction of tensile stresses from 50 to 300 days were 18.06 and 14.67%, and from 150 to 300 days were 14.17 and 7.30% for CG and KG FRP hybrid composite samples, respectively. The reduction in tensile stresses was gradually caused by continuous aging of both composites, due to weak fiber-matrix interfacial bonding. Fig. 10 further establishes that fiber pull-out, fiber-matrix debonding and fiber break were the main damage mechanisms responsible for the reduction of their mechanical properties at elevated temperature and long period of immersion. Consequently, they caused the degradation and failure of the hybrid composite samples. When compared with KG FRP composite samples, the aforementioned damage responses were lower in CG FRP composites, which depicted the reason behind their higher mechanical properties.

In addition, Fig. 8(b) shows the tensile properties of both composites at 40 °C. After 50 days of aging, the tensile stresses of both CG and KG FRP hybrid composites were 332.83 and 253.72 MPa, respectively. The rate of reduction in tensile stresses of aged CG and KG FRP hybrid composites were nearly 2.27 and 20.12%, respectively (Fig. 9b). The graphs significantly show that the tensile stresses of KG composites suddenly reduced, due to an increase in their times of exposure. After 150 days, the tensile stresses of both CG and KG FRP hybrid composites were 297.54 and 232.35 MPa, respectively. The rate of reduction in tensile stresses of aged CG and KG FRP hybrid composites were approximately 12.60 and 26.85% respectively (Fig. 9b), when compared with the dry composites. The percentage differences between 50 and 150 days were 10.6 and 8.4% for CG and KG FRP hybrid composites, respectively. After 300 days, the tensile stresses of aged CG and KG FRP hybrid composites were 254.82 and 214.89 MPa, respectively. The rate of reduction of tensile stresses of aged CG and KG FRP hybrid composites were almost 25.18 and 32.34%, respectively (Fig. 9b) when compared with the dry composites. The percentage reduction of tensile stresses from 50 to 300 days were 10.6 and 8.4%, and from 150 to 300 days were 14.35 and 7.5% for CG and KG FRP hybrid composites, respectively. The rate of reduction of tensile stress of KG FRP hybrid composite was less than that of CG FRP hybrid counterparts. The smaller tensile stress reduction recorded by CG composites was caused by lower water uptakes (Fig. 10).

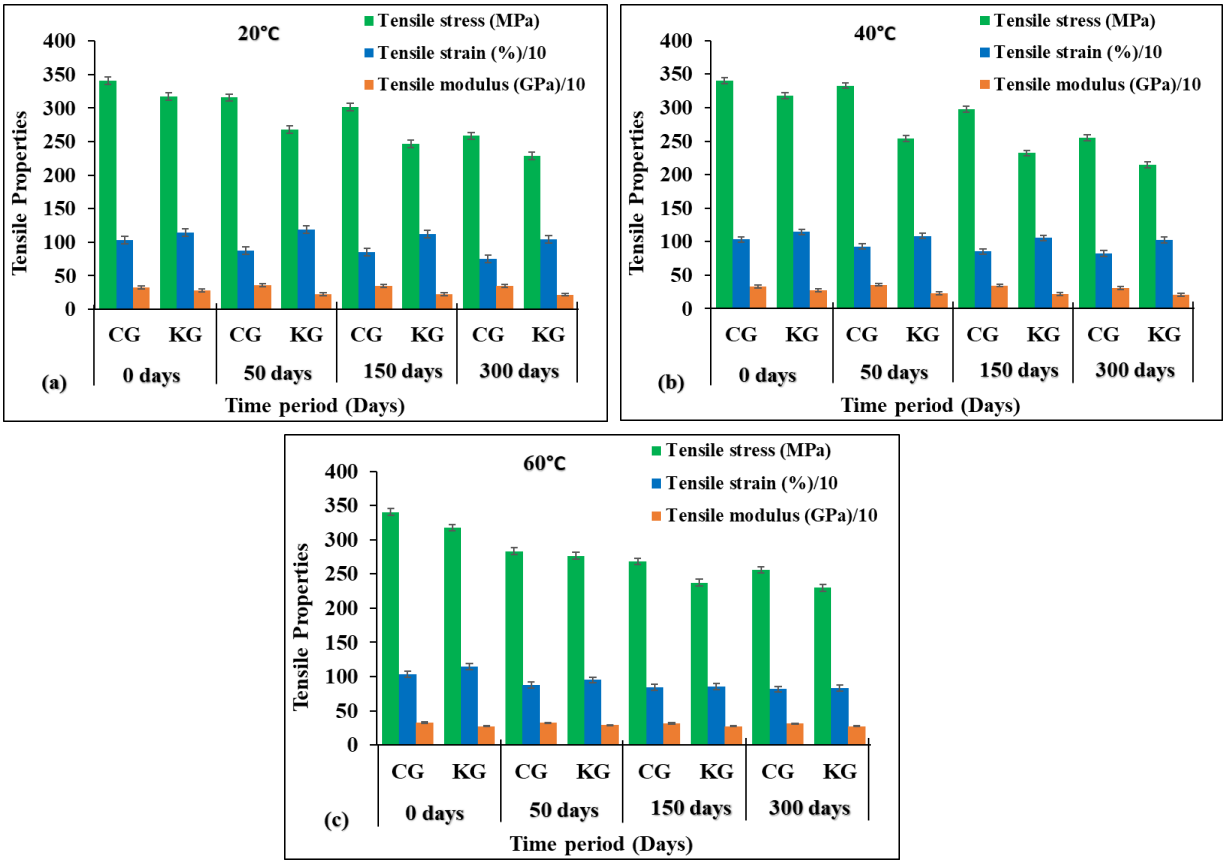

Fig. 8. Tensile properties of CG and KG FRP composite samples immersed in water at (a) 20, (b) 40 and (c) 60 °C.

Fig. 8(c) shows the tensile properties of both composites at 60 °C. After 50 days of aging, the tensile stresses of both CG and KG FRP hybrid composites were 283.40 and 276.51 MPa, respectively. The rate of reduction from aged CG and KG FRP hybrid composites were nearly 16.79 and 12.94%, respectively (Fig. 9c). The graphs unambiguously show that the tensile stresses of CG composites gradually reduced, due to an increase in their time of exposure. After 150 days, the tensile stresses of aged CG and KG FRP hybrid composites were 268.28 and 237.33 MPa, respectively. The rate of reduction of tensile stresses of aged CG and KG FRP hybrid composites were almost 21.22 and 25.28% (Fig. 9c) respectively, when compared with the dry composites. The percentage differences between 50 and 150 days were 5.33 and 14.17% for CG and KG FRP hybrid composites, respectively. After 300 days, the tensile stresses of aged CG and KG FRP hybrid composites were 255.97 and 230.09 MPa, respectively. The rate of reduction of tensile stresses were almost 24.84 and 27.56% for CG and KG FRP hybrid composites (Fig. 9c) respectively, when compared with the dry composites. The percentage reduction of tensile stresses from 50 to 300 days were 9.67 and 16.78%, and from 150 to 300 days were 4.59 and 3.05% for CG and KG FRP hybrid composites, respectively. The reduction of tensile stresses of KG FRP hybrid composites were faster

than that of CG counterparts. The graphs clearly show that the tensile stresses of aged composites constantly reduced, due to an increase in their time of exposure for all environments. The main cause of reduction in mechanical properties of the aged composites can be aatributed to the combined effects of moisture content or water absorption and exposure of the composites at elevated temperatures [37,38], such as 60 °C (Fig. 10).

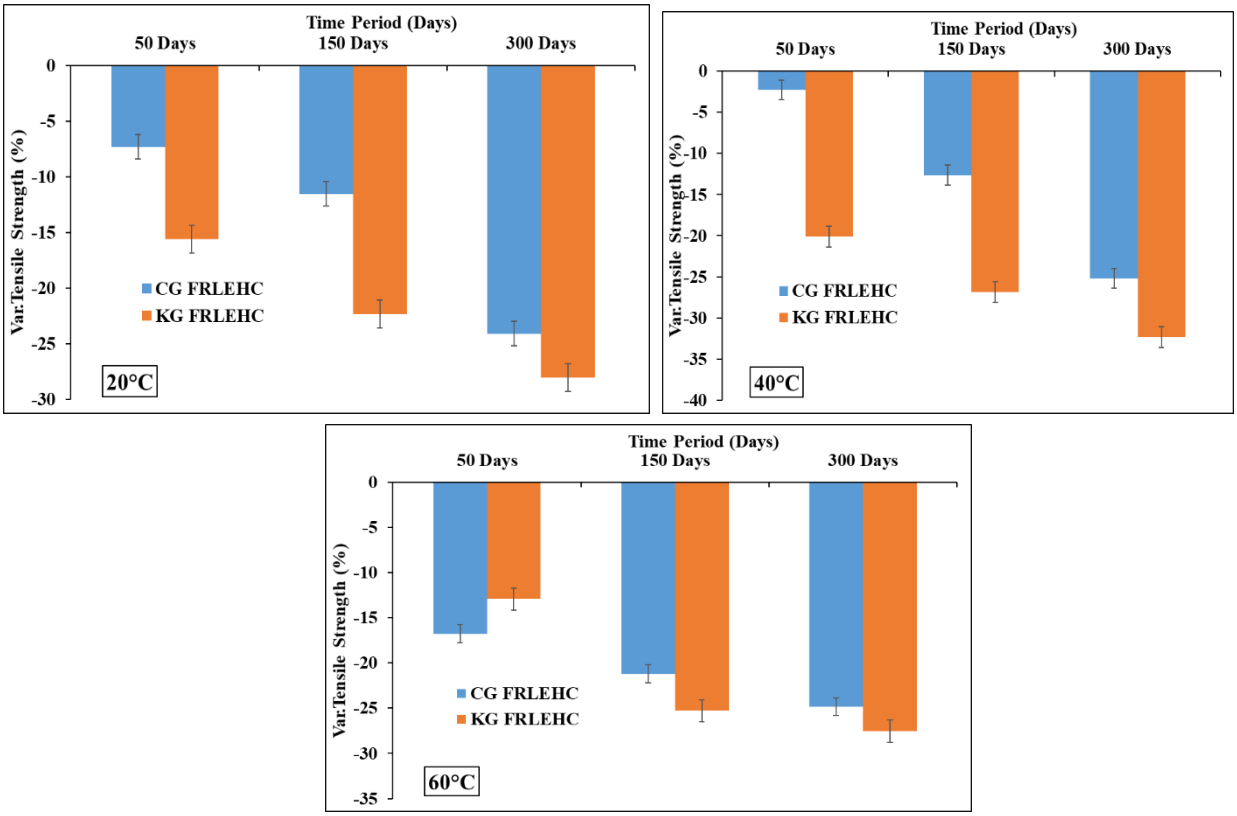

Fig. 9. Variable tensile strengths *versus* aging periods of CG and KG FRP hybrid composite samples immersed in water at (a) 20, (b) 40 and (c) 60 °C.

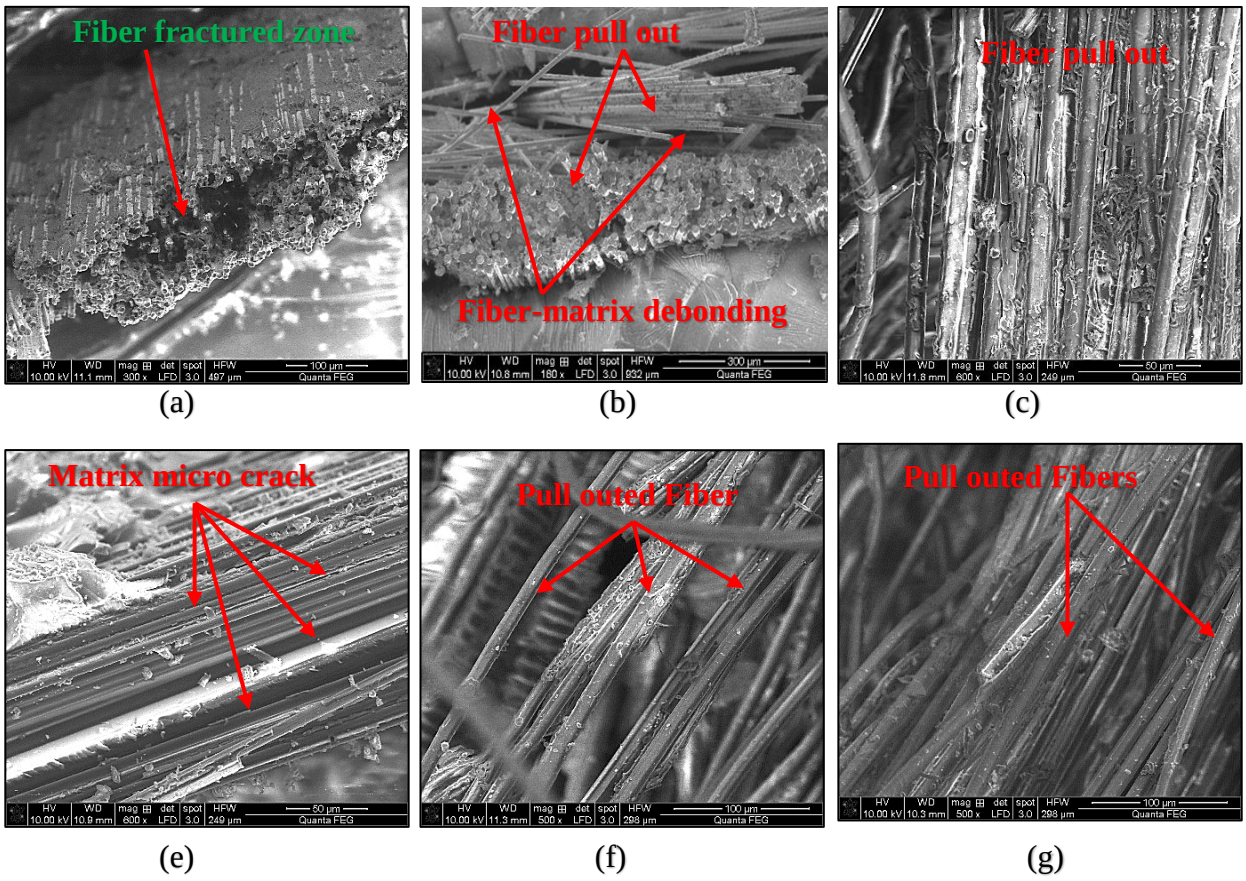

Fig. 10. Tensile fractured images of samples at 60 °C with 150 days aged (a, e, g) CG and (b, c, f) KG hybrid composites.

At 20 and 40 °C, Fig. 8 shows that the tensile moduli of the aged CG composites for all the aging periods were obtained higher when compared with the dry composites; with 0 day, but the moduli of aged CG composites at 60 °C were observed lower, due to weak fiber-matrix bonding and collapse of chemical bonding of matrix at higher temperature. The tensile strain also showed similar trend. In all environmental conditions, Fig. 8 shows that the tensile moduli of the aged KG composites for all aging periods were less, when compared with the dry composites. Also, the tensile strain gradually reduced by increasing the aging temperature and period. The tensile moduli of CG composites were observed higher for all aging periods and temperatures, due to the stronger carbon-epoxy-glass interfacial adhesion when compared with that of Kevlar-epoxy-glass FRP hybrid composites.

3.3. Prediction of apparent diffusion coefficient and activation energy

Table 3 presents the diffusion coefficients of CG and KG FRP hybrid composites at different temperatures. Eq. 7 was used to calculate the diffusion coefficients, with varied aging temperature and period. Both FRP hybrid composites recorded lowest values of diffusion coefficients at aging

temperature of 40 °C. Hence, the rates of reduction of tensile stresses and degradation of both composite samples were less when compared with other cases. From CG FRP hybrid composites, the percentage differences of diffusion coefficients between temperatures were 3.8% (20 – 40 °C), 28.57% (40 – 60 °C) and 25.71% (20 – 60 °C). Also, the percentage differences of diffusion coefficients between temperatures of KG FRP hybrid composites were 22.5% (20 – 40 °C), 37.5% (40 – 60 °C) and 23.43% (20 – 60 °C), respectively. By comparing diffusion coefficients of both composite samples, CG composites recorded lower values, while KG composites exhibited higher values at all aging temperatures. This is the main reason behind faster reduction of tensile strengths of KG composites than CG composites, hence accelerating the degradation process of the composite samples as quick as possible.

Table 3

Diffusion coefficients for CG and KG FRP hybrid composites at different aging temperatures.

FRP hybrid composites	Diffusion coefficient × 10^{-7} (mm^2/sec)		
	20 °C	40 °C	60 °C
CG	0.26	0.25	0.35
KG	0.49	0.40	0.64

Fig. 11 shows the plot of *ln(D) versus* inverse of temperature ($\frac{1}{T}$) in Kelvin. It was used to calculate E_a of CG and KG FRP hybrid composite samples, in addition to Eqs (5), 6 and 7. From Fig. 11, the coefficients of correlation, R^2 of CG and KG composites were greater than 0.98 (R^2> 0.98), which showed higher reliability. The slope of the line was measured from straight-line equation of both composites and it was multiplied with R value to obtain the E_a. Therefore, the predicted E_a was highly suitable for analyzing the behaviors of the composites. Table 4 presents the E_a of CG and KG FRP hybrid composite samples. It was evident that E_a of CG composite was higher than KG composite. The obtained lower E_a of KG composite indicated higher moisture absorption and higher matrix degradation of KG composite. This was similarly observed from the reduction of tensile stress of KG composite sample in Fig. 9. Hence, it provided a slightly lower long-term mechanical performance. On the contrary, CG composite exhibited better long-term mechanical performance, which can be attributed to lower moisture absorption and lower matrix degradation.

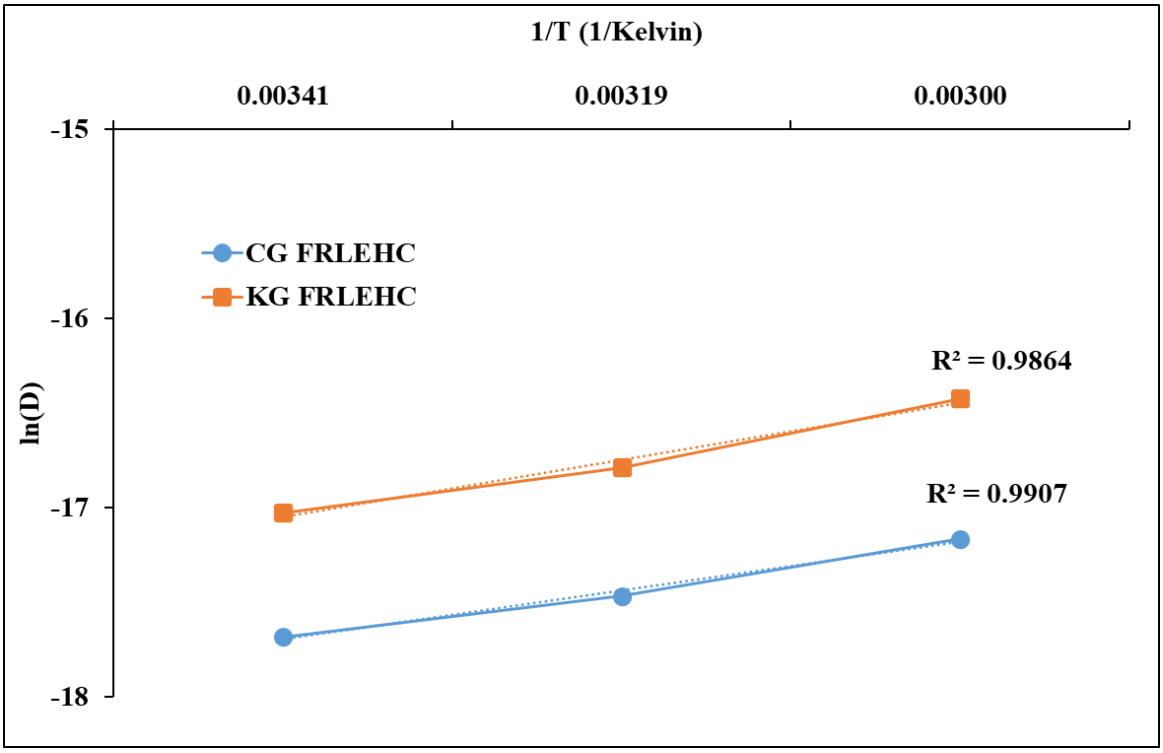

Fig. 11. Activation energies of both CG and KG FRP hybrid composites.

Table 4

Activation energy of FRP hybrid composites

FRP hybrid composites	Activation energy, E_a (kJ/mol)
CG	577.324
KG	432.993

3.4. Arrhenius plots

The Arrhenius principle [33] states that the occurrence of chemical degradation is dependent on the temperatures. This principle was effectively used to predict the long-term mechanical performance of the hybrid composites [1,29]. Fig. 12 shows the experimental tensile strength retention curves of CG and KG FRP hybrid composites. R^2 of CG FRP hybrid composite were higher values; greater than 0.98. This indicated slower material degradation and it can be used for a longer service life (Fig. 12a). R^2 values of KG composite were slightly lower than that of CG FRP hybrid composites, as depicted in Fig. 12(b). Therefore, KG FRP hybrid composites recorded a lower long-term performance when compared with CG composites. Overall, the R^2 values were observed to be highest for aged composites at 40 °C.

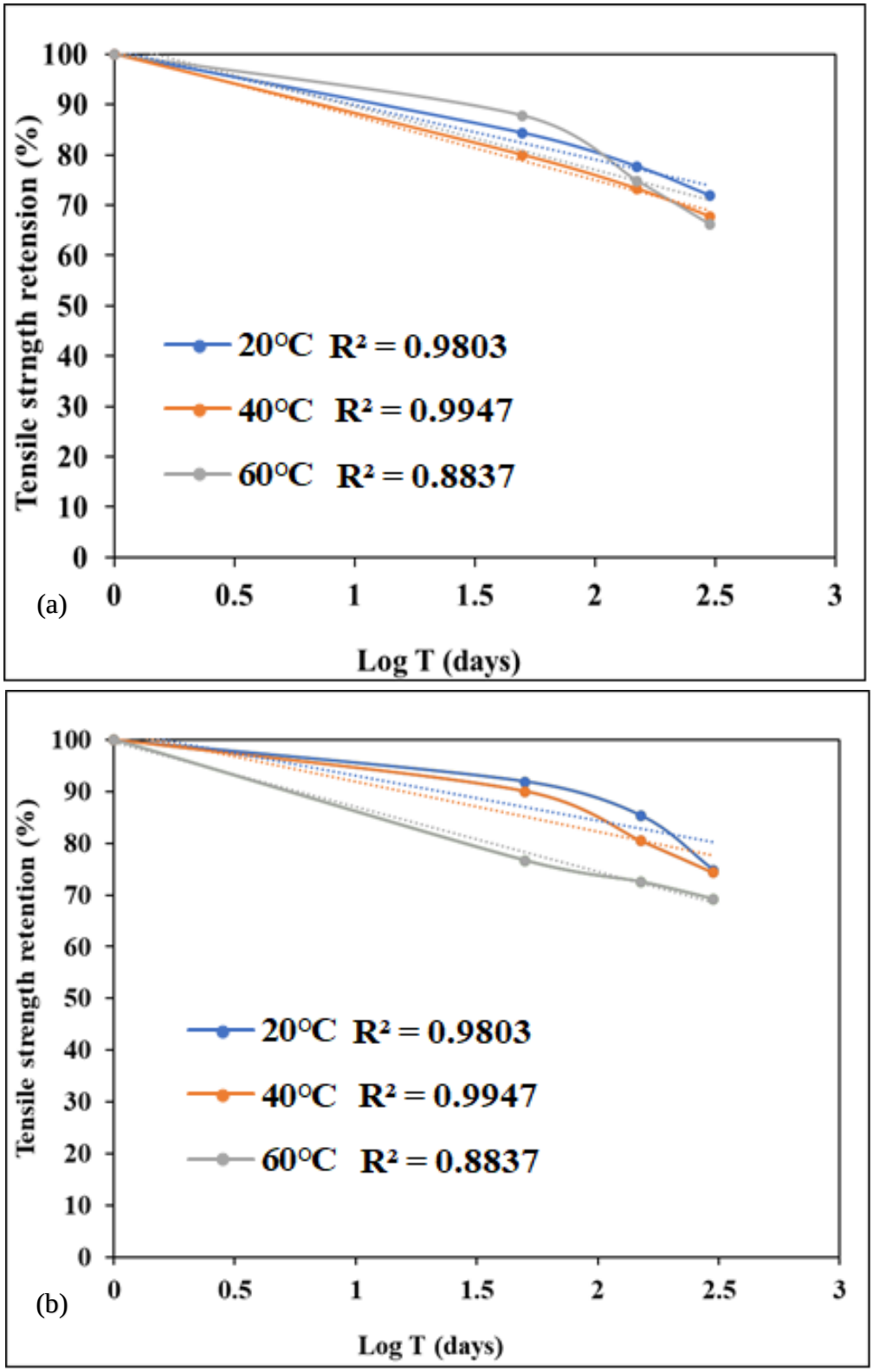

Fig. 12. Tensile strength retention *versus* aging period of (a) CG and (b) KG FRP hybrid composites at different aging temperatures.

Fig. 13 shows Arrhenius plots of the aged composites. The values obtained from regression line equations (Fig. 12) and selected service life of the materials were used to plot the curves at different service temperatures. Maximum of 20 years was selected to plot the curves by increasing one-year

interval (Fig. 13). From the plot, the maximum tensile stress retention was used to predict the service life of the composites. Furthermore, Fig. 14 shows the tensile stress retention *versus* service life of 100 years of CG and KG FRP hybrid composites. This helps to identify the strength pattern at any point of time. The value of tensile stress retention for a specific application can be identified, using desired period when minimal acceptable value is known for the application. Precisely, the maximum tensile stress retention was observed from the aged composites at 40 °C.

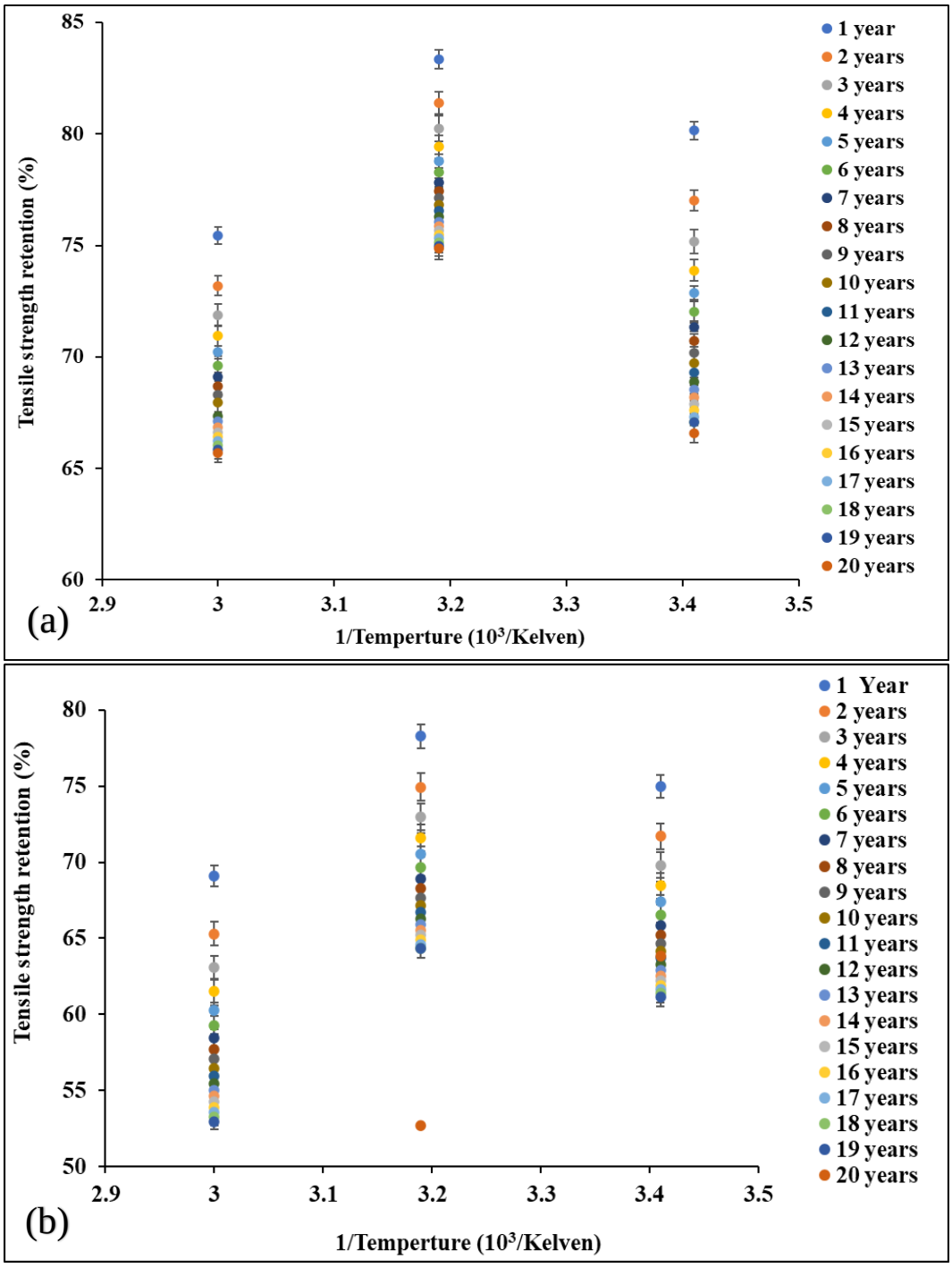

Fig. 13. Arrhenius plots of tensile strength retention against different temperatures of (a) CG and (b) KG FRP hybrid composites for 20 years.

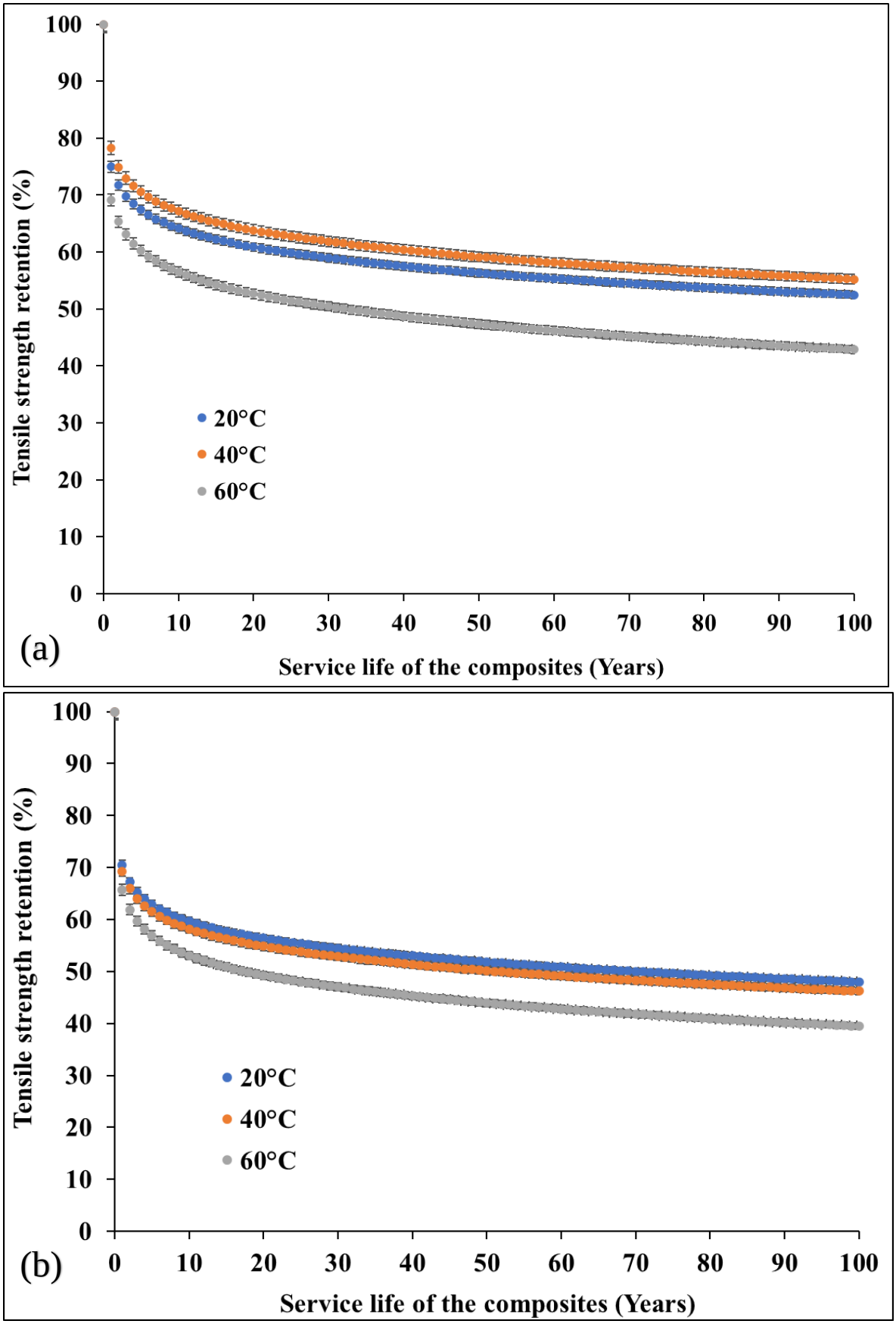

Fig. 14. Arrhenius plots of tensile strength retention *versus* service life of (a) CG and (b) KG FRP hybrid composites for 100 years.

3.5. Prediction of service life of CG and KG FRP hybrid composites

An appropriate average temperature was selected and used to predict the long-term performance of CG and KG composites under aged environments and also to calculate the tensile stress retention. This temperature is called average service temperature of the composites.

From Figs 13(a) and (b), considering first year service life of the aged composites, the average temperature was predicted from the linear fitting of regression equation. Therefore, the calculated average temperatures were 26.0 and 27.3 °C for CG and KG FRP hybrid composite, respectively. From literature survey, the average temperature of 23 °C was proposed for E-glass/vinyl ester composites by Carra and Carvelli [37,38]. Table 5 presents higher theoretical degradation values obtained from Arrhenius plots than natural water aging. This was purely based on greater degradation rate or higher temperature environment than the retention obtained in dry condition [1,16,30]. The tensile stress retention of CG and KG FRP hybrid composites at different times were obtained at 26.0 and 27.3 °C. The tensile stress retention after 1 year of normal water aging is shown in the bracket. The CG FRP hybrid composite exhibited higher retention of approximately 92% than the KG FRP hybrid composite of nearly 89% at normal water or natural aging.

Also, Table 5 depicts that faster rate of tensile stress degradation was obtained in the first year of exposure, while the rate of degradation of aged composites was consistently reduced by increasing their aging years continuously. These observations fully supported Fickian behaviors of both FRP hybrid composite samples, based on initial moisture observation of both composites and reaching a saturation stage/period, which reduced their degradation rates [1,31]. Similar experimental results have been reported on seawater durability and behaviors of epoxy/vinyl ester reinforced with glass/carbon composites of carbon/epoxy laminated composites [31].

Table 5

Predicted theoretical values of the tensile stress retention of CG and KG FRP hybrid composites at average temperatures.

Year	Tensile stress retention of CG FRP hybrid composite at 26.0 °C.	Tensile stress retention of KG FRP hybrid composite at 27.3 °C.
1	78.00 ±1.87 (≃92%)	77.00±2.15 (≃89%)
2	73.68±2.01	72.70±1.87
5	68.34±1.93	67.40±1.15
10	65.05±1.66	64.14±1.06
20	61.76±1.45	60.88±1.29
40	58.35±1.29	57.49±0.97
50	57.17±1.17	56.32±1.05
60	56.18±1.38	55.34±0.87
75	54.95±1.11	54.12±0.69
100	53.30±1.25	52.48±20.72

4. Conclusions

The present work involved fabrication of CG and KG FRP hybrid composite samples, using both hand layup and compression molding processes. The samples were immersed in water at different temperatures of 20, 40 and 60 °C. The long-term tensile performances of CG and KG FRP hybrid composites were analyzed by applying Arrhenius relationships to calculate the degradation of the composites at short periods of 50, 150 and 300 days.

The tensile stresses of CG FRP hybrid composites showed lower reduction when compared with KG FRP hybrid composites. The tensile stress retention gradually reduced during the first 50 days of aging in water. A progressive reduction in tensile stress was observed after 150 and 300 days. During these periods, both FRP hybrid composites absorbed higher water, hence they started exhibiting fiber-matrix debonding. The diffusion coefficients were higher at temperatures of 20 and 60 °C, due to an increase in water absorption coupled with debonding effect.

At 40 °C, the diffusion coefficients were observed to be lower, due to less water infusion. The activation energies of the aged composites were estimated, which were higher in CG FRP hybrid composites than KG composite counterparts. The calculated average aging temperatures for both

CG and KG FRP hybrid composites were 26.0 and 27.3 °C. These are the operating temperatures for both composites for longer durability and better service life. Arrhenius model was estimated over reduction of tensile stress. By setting 55% of tensile stress retention, the service life of the CG FRP hybrid composite was more than 70 years, while KG FRP hybrid composite recorded more than 55 years.

Finally, based on the aforementioned behaviors, both CG and KG FRP hybrid composites have promising future and potentials to be selected for various suitable structural/engineering applications, especially in marine, wind/tidal turbine, automobile and aerospace industries, among others.

References

[1] G. Kretsis, A review of the tensile, compressive, flexural and shear properties of hybrid fibre-reinforced plastics, Composites. 18 (1987) 13–23.

[2] A. Atiqah, Characterization and Interface of Natural and Synthetic Hybrid Composites, Elsevier Ltd., 2020. https://doi.org/10.1016/B978-0-12-803581-8.10805-7.

[3] M. Megahed, D.E. Tobbala, M.A.A. El-baky, The effect of incorporation of hybrid silica and cobalt ferrite nanofillers on the mechanical characteristics of glass fiber-reinforced polymeric composites, Polym. Compos. 42 (2021) 271–284.

[4] S.P. Kuruvilla, N.M. Renukappa, B. Suresha, Dynamic mechanical properties of glass fiber reinforced epoxy composites with micro and nanofillers, in: Techno-Societal 2018, Springer, 2020: pp. 337–347.

[5] P.P. Naidu, G. Raghavendra, S. Ojha, B. Paplal, Effect of g-C3N4 nanofiller as filler on mechanical properties of multidirectional glass fiber epoxy hybrid composites, J. Appl. Polym. Sci. 137 (2020) 48413.

[6] A.-H.I. Mourad, A.H. Idrisi, N. Zaaroura, M.M. Sherif, H. Fouad, Damage assessment of nanofiller-reinforced woven kevlar KM2plus/Epoxy resin laminated composites, Polym. Test. 86 (2020) 106501.

[7] R.K. Nayak, K.K. Mahato, B.C. Routara, B.C. Ray, Evaluation of mechanical properties of Al2O3 and TiO2 nano filled enhanced glass fiber reinforced polymer composites, J. Appl. Polym. Sci. 133 (2016).

[8] R. Gholami, H. Khoramishad, L.F.M. da Silva, Glass fiber-reinforced polymer nanocomposite adhesive joints reinforced with aligned carbon nanofillers, Compos. Struct.

253 (2020) 112814.

[9] S. Sharma, J. Rawal, S.R. Dhakate, B.P. Singh, Synergistic bridging effects of graphene oxide and carbon nanotube on mechanical properties of aramid fiber reinforced polycarbonate composite tape, Compos. Sci. Technol. 199 (2020) 108370.

[10] K.S. Unnikrishnan, T.S. Jose, K.J. Arun, Glass fiber reinforced bismaleimide/epoxy BaTiO3 nano composites for high voltage applications, Polym. Test. 87 (2020) 106505.

[11] R.K. Nayak, B.C. Ray, Influence of seawater absorption on retention of mechanical properties of nano-TiO 2 embedded glass fiber reinforced epoxy polymer matrix composites, Arch. Civ. Mech. Eng. 18 (2018) 1597–1607.

[12] R.K. Nayak, B.C. Ray, Retention of mechanical and thermal properties of hydrothermal aged glass fiber-reinforced polymer nanocomposites, Polym. Plast. Technol. Eng. 57 (2018) 1676–1686.

[13] R.K. Nayak, K.K. Mahato, B.C. Ray, Water absorption behavior, mechanical and thermal properties of nano TiO2 enhanced glass fiber reinforced polymer composites, Compos. Part A Appl. Sci. Manuf. 90 (2016) 736–747.

[14] T.S.M. Kumar, K. Senthilkumar, M. Chandrasekar, S. Subramaniam, S.M. Rangappa, S. Siengchin, N. Rajini, Influence of fillers on the thermal and mechanical properties of biocomposites: an overview, Biofibers Biopolym. Biocomposites. (2020) 111–133.

[15] Y. Yu, X. Yang, L. Wang, H. Liu, Hygrothermal aging on pultruded carbon fiber/vinyl ester resin composite for sucker rod application, J. Reinf. Plast. Compos. 25 (2006) 149–160.

[16] Y. Yu, P. Li, G. Sui, X. Yang, H. Liu, Effects of hygrothermal aging on the thermal–mechanical properties of vinylester resin and its pultruded carbon fiber composites, Polym. Compos. 30 (2009) 1458–1464.

[17] A. Dogan, C. Atas, Variation of the mechanical properties of E-glass/epoxy composites subjected to hygrothermal aging, J. Compos. Mater. 50 (2016) 637–646.

[18] A.P.C. Barbosa, A.P.P. Fulco, E.S.S. Guerra, F.K. Arakaki, M. Tosatto, M.C.B. Costa, J.D.D. Melo, Accelerated aging effects on carbon fiber/epoxy composites, Compos. Part B Eng. 110 (2017) 298–306.

[19] L. Liu, Z. Zhao, W. Chen, C. Shuang, G. Luo, An experimental investigation on high velocity impact behavior of hygrothermal aged CFRP composites, Compos. Struct. 204 (2018) 645–

657.

[20] M. Johar, W.W.F. Chong, H.S. Kang, K.J. Wong, Effects of moisture absorption on the different modes of carbon/epoxy composites delamination, Polym. Degrad. Stab. 165 (2019) 117–125.

[21] K. Senthilkumar, T. Ungtrakul, M. Chandrasekar, T.S.M. Kumar, N. Rajini, S. Siengchin, H. Pulikkalparambil, J. Parameswaranpillai, N. Ayrilmis, Performance of Sisal/Hemp Bio-based Epoxy Composites Under Accelerated Weathering, J. Polym. Environ. (2020) 1–13.

[22] S. Ma, Y. He, L. Hui, L. Xu, Effects of hygrothermal and thermal aging on the low-velocity impact properties of carbon fiber composites, Adv. Compos. Mater. 29 (2020) 55–72.

[23] M. Raji, N. Zari, R. Bouhfid, Durability of composite materials during hydrothermal and environmental aging, in: Durab. Life Predict. Biocomposites, Fibre-Reinforced Compos. Hybrid Compos., Elsevier, 2019: pp. 83–119.

[24] T. Liu, X. Liu, P. Feng, A comprehensive review on mechanical properties of pultruded FRP composites subjected to long-term environmental effects, Compos. Part B Eng. 191 (2020) 107958.

[25] G. Quino, V.L. Tagarielli, N. Petrinic, Effects of water absorption on the mechanical properties of GFRPs, Compos. Sci. Technol. 199 (2020) 108316.

[26] S.F.M. Asasaari, K.J. Wong, M.N. Tamin, M. Johar, Moisture absorption effects on the mechanical properties of carbon/epoxy composites, Int. J. Struct. Integr. (2020).

[27] C. Javier, J. LeBlanc, A. Shukla, Hydrothermally degraded carbon fiber/epoxy plates subjected to underwater explosive loading in a fully submerged environment, Mar. Struct. 72 (2020) 102761.

[28] A.N. Rajaram, C.G. Boay, N. Srikanth, Effect of curing on the hygrothermal behaviour of epoxy and its carbon composite material, Compos. Commun. 22 (2020) 100507.

[29] L. Xu, Y. He, S. Ma, L. Hui, Y. Jia, Y. Tu, Effects of aging process and testing temperature on the open-hole compressive properties of a carbon fiber composite, High Perform. Polym. 32 (2020) 693–701.

[30] A. Kootsookos, A.P. Mouritz, Seawater durability of glass-and carbon-polymer composites, Compos. Sci. Technol. 64 (2004) 1503–1511.

[31] H.N. Narasimha Murthy, M. Sreejith, M. Krishna, S.C. Sharma, T.S. Sheshadri, Seawater

durability of epoxy/vinyl ester reinforced with glass/carbon composites, J. Reinf. Plast. Compos. 29 (2010) 1491–1499.

[32] L. Bian, J. Xiao, J. Zeng, S. Xing, Effects of seawater immersion on water absorption and mechanical properties of GFRP composites, J. Compos. Mater. 46 (2012) 3151–3162.

[33] H. Xin, Y. Liu, A. Mosallam, Y. Zhang, Moisture diffusion and hygrothermal aging of pultruded glass fiber reinforced polymer laminates in bridge application, Compos. Part B Eng. 100 (2016) 197–207.

[34] A. Anand, S.K. Ghosh, R.K. Prusty, Effects of seawater absorption and desorption on the long-term creep performance of graphene oxide embedded glass fiber/epoxy composites, Polym. Compos. 41 (2020) 4861–4871.

[35] Y. Zhong, M. Cheng, X. Zhang, H. Hu, D. Cao, S. Li, Hygrothermal durability of glass and carbon fiber reinforced composites–A comparative study, Compos. Struct. 211 (2019) 134–143.

[36] D.K. Jesthi, R.K. Nayak, Evaluation of mechanical properties and morphology of seawater aged carbon and glass fiber reinforced polymer hybrid composites, Compos. Part B Eng. 174 (2019) 106980.

[37] G. Carra, V. Carvelli, Long-term bending performance and service life prediction of pultruded Glass Fibre Reinforced Polymer composites, Compos. Struct. 127 (2015) 308–315.

[38] G. Carra, V. Carvelli, Aging of pultruded glass fibre reinforced polymer composites exposed to combined environmental agents, Compos. Struct. 108 (2014) 1019–1026.

[39] A. Zafar, F. Bertocco, J. Schjodt-Thomsen, J.C. Rauhe, Investigation of the long term effects of moisture on carbon fibre and epoxy matrix composites, Compos. Sci. Technol. 72 (2012) 656–666.

[40] A.C.D.-30 on C. Materials, Standard test method for tensile properties of polymer matrix composite materials, ASTM international, 2008.